DESIGN AND FABRICATION OF A NOVEL THERMALLY-ACTUATED NO ELECTRIC POWER EVENT-DRIVEN MEMS SENSOR FOR IOT APPLICATIONS

Dilan Ratnayake[1*] *and Kevin M. Walsh*[1]
[1]University of Louisville, Louisville, Kentucky, USA

ABSTRACT

This paper introduces the emerging field of no-electrical-power (NEP) event-driven sensing as a potential solution to the anticipated energy challenges posed by the growth and proliferation of IoT devices. A novel approach is presented that utilizes smart-engineered bistable multilayers to create environmentally sensitive sensors that consume zero electrical power. Building upon our previous research on released multi-layer bistable films, this study demonstrates how they can be innovatively used as the fundamental sensing element for NEP environmental sensors. Through careful mechanical design modeling and fine control of fabrication processing conditions, we show it is feasible to create autonomous bistable NEP devices that achieve successful thermal actuation to specific environmental temperature conditions. Furthermore, each diaphragm design has its own unique snapping temperature identifier consistent with its layout design, material selection, and processing conditions. The findings pave the way for the development of a new wave of MEMS-based no-power event-driven smart switches that help fulfill the promise of the ever-growing and ever-expanding Internet of Things.

KEYWORDS

MEMS, no-electrical-power, IoT, event-driven, bistable, buckle, environmental sensing, thermal actuation.

INTRODUCTION

With the exponential growth of the Internet of Things (IoT) anticipated to reach a trillion devices worldwide by 2035 [1], there arises a pressing concern regarding the energy demands, consumption, and conservation strategies for these pervasive sensing devices. Addressing this challenge necessitates a fundamental reevaluation of sensor design paradigms, ushering in the potential for a new era of zero-electrical-power (NEP) event-driven sensing. This paper delves into the nascent field of NEP sensing, offering crucial insights into its principles, designs, material selection, processing conditions, and applications. Building upon our team's prior advancements in bistable bilayer films [2-4], this research introduces the innovative utilization of released tri-layer films as the foundation for NEP sensors, particularly focusing on MEMS-based bistable environmental sensing. Key to the success of these NEP sensors is the careful design and selection of the tri-layer films. We demonstrate the use of thermal oxide as a compressive layer, polyimide as a thick structural layer, and aluminum with its intentionally mismatched temperature expansion coefficient (TEC) as the active layers. Through detailed mechanical modeling and precise fabrication processing, we demonstrate repeatable and reliable bistable behavior and effective thermal actuation, laying the groundwork for the development of MEMS-based no-power smart switches. This introduction sets the stage for a comprehensive exploration of NEP event-driven sensing, elucidating its potential to revolutionize the landscape of IoT devices and energy-efficient sensor technologies.

BUCKLING CRITERIA FOR CIRCULAR DIAPHRAGMS

Buckling is a mechanical phenomenon possible in structures like beams and diaphragms that is related to compressive stress, material stiffness, and the structure's slenderness ratio [5]. Initially, when lateral compressive forces are applied to an object like a diaphragm for example, it undergoes simple compression with little lateral displacement. However, as the compressive stress increases, the structure can become unstable. Upon reaching the critical buckling stress, the diaphragm rapidly deflects transversely and buckles to its first stable state, which has a lower strain energy than the compressed state [4, 6, 7]. This phenomenon occurs in large structures and can also occur with miniature devices fabricated using MEMS technology. If enough internal compressive stress is present during thin film deposition (due for example to mismatched thermal expansion coefficients during growth) the thin films will buckle upon their release. These miniature buckled diaphragms can be effectively modeled using traditional mechanical engineering equations as shown below. Being able to model and accurately predict this behavior is crucial for designing MEMS-based bistable structures.

The effective internal compressive stress ($\sigma_{C_{eff}}$) needed to produce diaphragm buckling is given by [4]:

$$\sigma_{C_{eff}} = -\frac{4}{3}\frac{t^2}{R^2}\frac{Y_{eff}}{(1-v_{eff}{}^2)} \quad (1)$$

Where R is the radius of the circular diaphragm, t is the total thickness, Y_{eff} is the film's effective Young's Modulus and, v_{eff} is the film's effective Poisson Ratio.

The height of the buckled circular diaphragm structure (h_0) can be predicted using [4]:

$$h_0 = \pm\frac{\sqrt{35}}{4}t\sqrt{\frac{\sigma_{0_{eff}}}{-\sigma_{C_{eff}}} - 1} \quad (2)$$

Where $\sigma_{0_{eff}}$ is the effective residual stress.

For a bilayer film, we need to find the effective Young's Modulus, effective Poisson Ratio, and effective residual stress, considering the material properties of each film using the following equations [4].

$$Y_{eff} = \left(\frac{t_{film1}\times Y_{film1} + t_{film2}\times Y_{film2}}{t_{film1}+t_{filme2}}\right) \quad (3)$$

$$v_{eff} = \left(\frac{t_{film1}\times v_{film1} + t_{film2}\times v_{film2}}{t_{film1}+t_{film2}}\right) \quad (4)$$

$$\sigma_{0_{eff}} = \left(\frac{t_{film1}\times \sigma_{0_{film1}} + t_{film2}\times \sigma_{0_{film2}}}{t_{film1}+t_{film2}}\right) \quad (5)$$

Utilizing the above equations, we next designed an array of various-sized diaphragms to experimentally test our buckling theory. As shown in Fig. 1, the effective diaphragm stress needs to be larger than the critical stress for buckling if each element in our proposed array is to buckle. The critical stress was calculated using equation (1), and the effective residual stress was calculated using equation (5). The residual stress of each film was determined using a Toho stress analyzer. With these data, we were able to design an appropriate 6-element array consisting of 6 different diameter sizes,

978-1-940470-05-4/HH2024/$25©2024TRF
DOI 10.31438/TRF.HH2024.47

ranging from 800 µm to 1300 µm in 100 µm increments. As shown in Fig. 1, all 6 elements of our array should achieve the minimum standard for buckling. To test our theory, a photomask was designed containing the 6 different diameter designs.

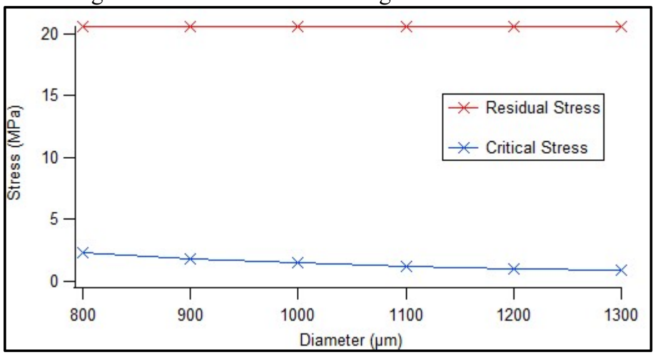

Figure 1: Effective residual stress and critical stress vs diaphragm diameter for 0.33µm oxide/4.0µm polyimide diaphragms.

FABRICATION PROCESS

Our fabrication process, illustrated in Fig. 2, starts with a double side polish 4" silicon wafer, cleaned using the RCA cleaning process as represented in Fig. 2(a). To establish a robust oxidation layer, we employed a dry/wet/dry thermal cycle, subjecting the wafer to 1.2 hours of oxidation at 1000℃ utilizing a three-zone tube furnace, as shown in Fig. 2 (b). After the oxidation process, the thickness of the oxide layer was measured using a Filmetrics system, revealing a measurement of 0.33 µm. This ultra-thin oxide layer plays a pivotal role in generating internal mechanical forces crucial for inducing buckling in subsequent circular structures upon release.

Next, the structural layer was applied, as illustrated in Fig. 2(c). For our structural layer, we opted for PI-2611 polyimide, chosen for its high viscosity stemming from its elevated molecular weight, ensuring the necessary mechanical support. To guarantee the wafer's complete dryness, a dehydration bake was performed for two minutes at 115℃ on a hotplate, eliminating any residual moisture and preparing the surface for polyimide application. Subsequently, PI 2611 was spun onto the wafer, adjusting spread and spin parameters to achieve a 4.0 µm thick polyimide layer. Following the spin, a soft bake ensued using a hotplate set at 130℃ for an additional 3 minutes to eliminate any remaining solvent in the film. Following the soft bake, the wafer was transferred to a Yes Polyimide Oven, a high-temperature vacuum oven, for thermal curing. The absence of the PI layer results in fragile silicon dioxide layers, leading to wrinkled and imperfect "domes," as illustrated experimentally in Fig. 3. Moreover, the thickness of the PI layer enables precise adjustment of the switching thresholds and heights of the bistable devices, thus augmenting their functionality.

Following the deposition of polyimide/oxide structural layer, the wafer was transferred to the lithography bay. Here, the designed 6-element arrays of circular patterns were opened on the backside of the wafer to facilitate the subsequent etching of bulk silicon using DRIE, resulting in the formation of diaphragms as represented in Fig. 2 (d). The process details are as follows: Initially, the wafer go through a dehydration bake on a hotplate at 115℃ for three minutes. Subsequently, AZ4620 photoresist was applied to the backside of the wafer via a spinner. This was followed by a soft bake conducted for 10 minutes at 100℃. Standard binary lithography was then carried out utilizing an MA6/BA6 Suss Mask Aligner, which supplied UV light for exposure, along with a photomask containing circular features ranging from 800 µm to 1300 µm diameter. Upon exposure to UV light, AZ400k Developer was used to develop the exposed structures. Then, a hard bake was performed by placing the patterned wafer on a hotplate at 115℃ for one minute, effectively removing any remaining solvents and enhancing the resist's ability to serve as an etch mask. Finally, the Buffer Oxide Etch (BOE) etch was done for around four minutes to etch the oxide.

The next step involved transferring the samples to the DRIE System for bulk silicon etching from the backside. The process continued until reaching the top etch stop layer, which was the thermally grown oxide film, as represented in Fig. 2(e). Subsequently, a Dektak profilometer was used to measure the depth of the etched structure. Upon the release of the diaphragm using DRIE, the internal compressive stress led the diaphragms to buckle into smooth and uniform domed structures, illustrated in Fig. 2(e). To observe the buckled profiles, an optical microscope, and a Dektak profilometer were used.

For thermal actuation, a thin layer of aluminum, approximately 350 nm in thickness, is selectively deposited using a shadow mask covering 50% and 60% of the diaphragm area using the Technics sputtering system (Fig. 2(f)). All diaphragms were set to their buckled-down state using a vacuum during the aluminum sputtering process. Leveraging the high TEC of the aluminum layer, it serves as the primary source for thermal actuation within the sensor system.

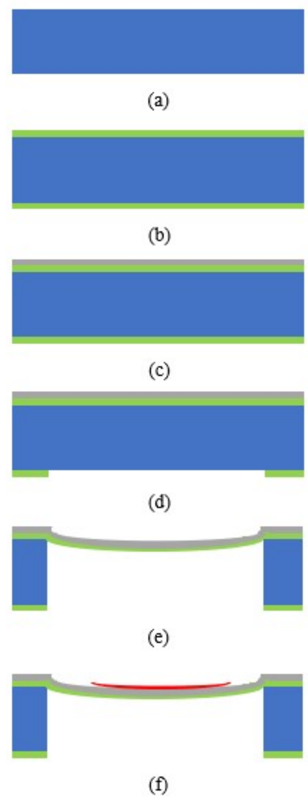

Figure 2: Fabrication process for producing oxide/PI/aluminum bistable diaphragms. (a) silicon wafer clean, (b) thermal oxidation, (c) spin polyimide film on frontside and thermally cure, (d) backside photolithography, (e) deep reactive ion etch of silicon to release the diaphragms and allow them to buckle, (f) use vacuum to set diaphragms to their buckled-down state followed by aluminum deposition through an aligned shadow mask.

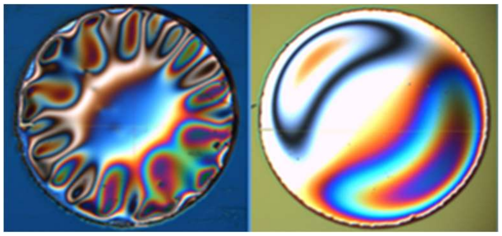

Figure 3: Optical image using DIC of a wrinkled buckled diaphragm vs a nice symmetric "wrinkle-free" version.

RESULTS AND DISCUSSION

Our released buckled diagrams not only demonstrate excellent bistable behavior but also serve as a foundational aspect of our research. In Fig. 4, we present the profiles of our device in both its "buckled up" and "buckled down" states, supplemented by images captured using DIC microscopy. This microscopic technique enables us to determine between the two states with precision. However, our exploration doesn't stop there. For a given film thickness and residual compressive stress, there exists a limited range of diaphragm diameters that display bistable behavior. This is because, as previously explained, the critical stress for buckling must always be lower than the effective residual stress in the multi-layer film. Using this as a baseline, we fabricated a 6-element array of various-sized diaphragms, ranging from 800 to 1300 µm in diameter, to confirm our theoretical predictions, as explained before. By employing equation (2), we developed a robust multi-layer model that accurately predicts the device's maximum buckling height. Figure 5 shows the close agreement between our theoretical predictions and experimental results, reaffirming the efficacy of our model and approach.

Finally, to demonstrate the feasibility of "programming" these bistable structures to autonomously respond to environmental conditions, such as temperature changes, we introduced a third "active" layer to the bistable diaphragm. As shown in Fig. 6, we carefully patterned aluminum diaphragms on top of the polyimide while the bistable elements were in their buckled-down state using a carefully aligned shadow mask. Aluminum was chosen for its significantly larger CTE compared to polyimide and silicon dioxide. Consequently, as the environmental temperature rises, the aluminum film expands, causing the device to transition from a "buckled-down" to a "buckled-up" state at a designated temperature. This interesting bistable 'snapping' behavior is demonstrated in Fig. 7 for a range of diaphragm diameters, with varying percentages of aluminum coverage. Each diaphragm configuration exhibits a unique snapping temperature identifier, ranging from 37°C to 118°C, consistent with its design and processing conditions.

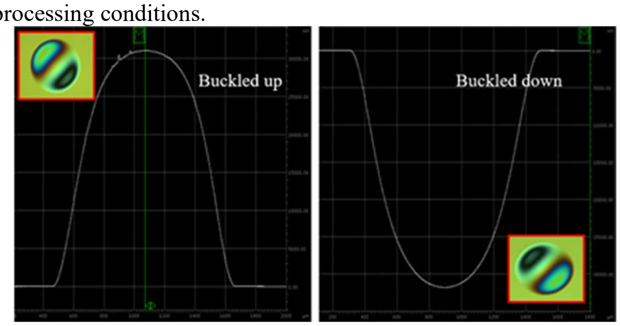

Figure 4: Profilometry data for diaphragms in Buckled Up and Buckled Down states. Insets show DIC optical images.

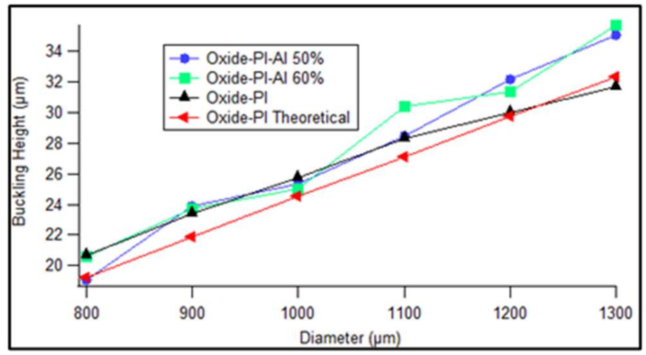

Figure 5: Comparison of experimental and theoretical buckling height vs. diaphragm diameter for 0.33µm oxide/4.0µm polyimide/ 0.35µm aluminum diaphragms.

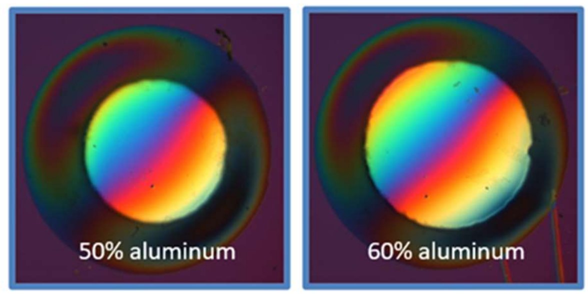

Figure 6: Aluminum discs patterned on top of the bistable structures while in their buckle-down state.

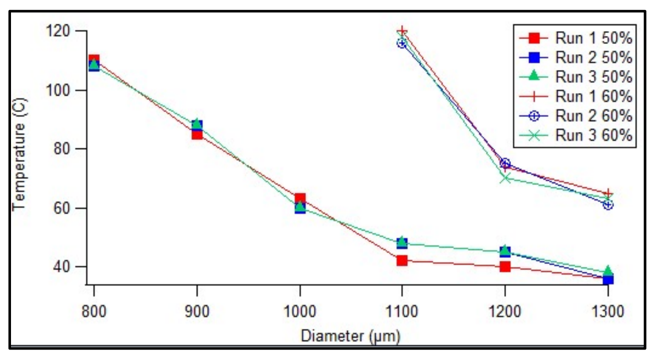

Figure 7: Comparison of 50% and 60% aluminum covered diaphragm's switching temperature vs. diaphragm diameter for 0.33µm oxide/4.0µm polyimide/ 0.35µm aluminum diaphragms.

CONCLUSION

This research developed the foundation for MEMS-based, no electrical power (NEP), event-driven, environmental sensors using smart tri-layer bistable diaphragms. We present the design considerations, material selection criteria, mechanical modeling, and fabrication control needed to develop functioning prototype devices. By carefully engineering compressive stress within the thermally grown oxide layer, we induced buckling in the released films. However, the delicate nature of the thin oxide necessitated a stress-free structural layer to ensure the formation of uniform hemispherical domes. Polyimide emerged as an ideal material for this structural layer. Aluminum, on the other hand, proved to be an excellent candidate for providing the necessary thermal actuation to induce its binary mechanical state change. Arrays of oxide-polyimide-aluminum tri-layer domes, with diameters ranging from 800 µm to 1300 µm, were fabricated and demonstrated mechanical bistability. All diaphragms were characterized, and their experimental buckling height data were compared with the theoretical model. Moreover, we are currently in the process of developing Finite Element Analysis (FEA) models to further compare experimental snapping temperature data. The theoretical model yielded predictions that closely matched experimental observations regarding buckling height. Finally, our ongoing efforts involve integrating the bistable mechanism into a functional MEMS no-power smart switch, as depicted in Fig. 8. This endeavor marks a significant step towards realizing efficient, autonomous, no electrical power (NEP) self-actuating MEMS-based sensors with broad applicability.

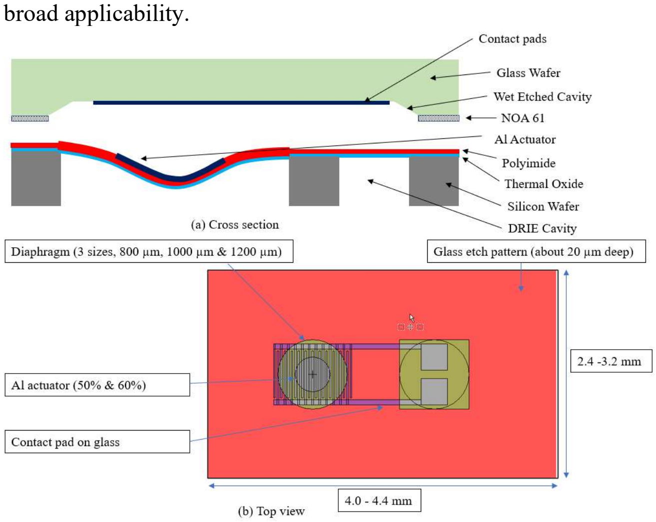

Figure 8: Design of the MEMS no-power smart switch: (a) Cross-section, and (b) Top view.

ACKNOWLEDGEMENTS

This research was partially funded by National Science Foundation under Award #2025075. The authors also wish to acknowledge the University of Louisville Micro/Nano Technology Centre (MNTC) and its cleanroom staff for their assistance with the many fabrication processes.

REFERENCES

1. Berger, I.W. *The Internet of Things Is Changing the World*. The Wall Street Journal 2020; Available from: https://www.wsj.com/articles/the-internet-of-things-is-changing-the-world-01578689806?tesla=y.
2. Gowrishetty, U.R., K.M. Walsh, and T.A. Berfield, *Fabrication of polyimide bi-stable diaphragms using oxide compressive stresses for the field of 'Buckle MEMS'.* Journal of Micromechanics and Microengineering, 2010. **20**(7): p. 075013.
3. Ratnayake, D., et al., *Engineering stress in thin films for the field of bistable MEMS.* Journal of Micromechanics and Microengineering, 2015. **25**(12): p. 125025.
4. Ratnayake, D., et al., *Bistability study of buckled MEMS diaphragms.* Journal of Physics Communications, 2020. **4**(10): p. 105008.
5. Gowrishetty, U.R., K.M. Walsh, and D. Jackson. *No-power vacuum actuated bi-stable MEMS SPDT switch*. in *SENSORS, 2010 IEEE*. 2010. IEEE.
6. Arya, R., et al., *Thermally actuated, bistable, oxide/silicon/metal membranes.* Journal of Micromechanics and Microengineering, 2005. **16**(1): p. 40.
7. Ding, X., et al. *A study on silicon-diaphragm buckling*. in *IEEE 4th Technical Digest on Solid-State Sensor and Actuator Workshop*. 1990.

CONTACT

*D. Ratnayake; d0ratn01@louisville.edu